

Positive contrast visualization for cellular magnetic resonance imaging using susceptibility-weighted echo-time encoding

Young Beom Kim^{a,b}, Ki Hyun Bae^c, Seung-Schik Yoo^d, Tae Gwan Park^c, HyunWook Park^{a,*}

^a*Division of Electrical Engineering, School of Electrical Engineering and Computer Science, KAIST, Daejeon 305-701, Republic of Korea*

^b*In-Vivo-NMR Laboratory, Max-Planck-Institute for Neurological Research, Cologne 50931, Germany*

^c*Department of Biological Sciences, KAIST, Daejeon 305-701, Republic of Korea*

^d*Department of Radiology, Harvard Medical School, Brigham and Women's Hospital, Boston, MA 02115, USA*

Received 10 December 2007; revised 11 September 2008; accepted 28 October 2008

Abstract

Objective: The objective of this study was to investigate a method to generate positive contrast, selective to superparamagnetic iron oxide (SPIO) labeled cells, using the susceptibility-weighted echo-time encoding technique (SWEET).

Materials and Methods: SPIO-labeled human epidermal carcinoma (KB) cells were placed in a gel phantom. Positive contrast from the labeled cells was created by subtraction between conventional spin-echo images and echo-time shifted susceptibility-weighted images. SPIO-labeled cells were injected into the left dorsal flank and hind limb of nude mice, and unlabeled cells were placed on the right side as controls. Tumor growth was monitored using the proposed method, and a histological analysis was used to confirm the presence of the labeled cells.

Results: Based on in vitro testing, we could detect 5000 labeled cells at minimum and the number of pixels with positive contrast increased proportionally to the number of labeled cells. Animal experiments also revealed the presence of tumor growth from SPIO-loaded cells.

Conclusions: We demonstrated that the proposed method, based on the simple principle of echo-time shift, could be readily implemented in a clinical scanner to visualize the magnetic susceptibility effects of SPIO-loaded cells through a positive-contrast mechanism.

© 2009 Elsevier Inc. All rights reserved.

Keywords: Iron oxide particles; Magnetic susceptibility; Positive contrast; In vivo cellular MRI; Tumor

1. Introduction

Recently, interest in noninvasive means for tracking/imaging cells, including stem cells, has increased due to the potential of the noninvasive assessment for regenerative medicine and cell-based therapies. Superparamagnetic iron oxide (SPIO) particles are commonly used to label cells for cellular imaging since they can be readily internalized into cells via co-culture with transfection agents [1] or via electroporation [2]. Through detecting the SPIO particles using MRI, in vivo imaging of implanted cells for cell replacement therapies has become feasible [3]. SPIO particles have primarily been employed to detect lesions in the liver [4] associated with alterations in the reticuloen-

dothelial system. The phagocytic Kupffer cells found in the liver, few of which are present in tumor tissue, have a characteristic tendency to ingest SPIO molecules. As a result, healthy liver cells and tumor cells exhibit different transverse relaxation rates (R_2) and can thus be visually distinguished in T_2 -weighted MR images [5].

SPIO-loaded cells disturb the local magnetic field near the cells, thereby dephasing the spins. Consequently, the cells are visualized as a signal void that is contrasted to a brighter background (i.e., negative contrast) [1,2]. A significant drawback that is typically associated with this negative contrast is that it can be confused with a low-level MR signal arising from adjacent tissues (such as bone or vasculature). In order to selectively detect SPIO-labeled cells in MR images, positive contrast with suppression of the background tissue is warranted [6].

Several methods to generate positive contrast of magnetically labeled cells have been suggested, including

* Corresponding author.

E-mail address: hwpark@athena.kaist.ac.kr (H. Park).

(1) spectrally selective excitation of an off-resonance region near the labeled cells [6]; (2) suppression of signals from nonlabeled regions by dephasing [7–9]; and (3) a spectroscopy-based method that encodes the off-resonance image and subsequently decomposes the signal into on-and-off resonance images [10]. In this work, we present a method whereby SPIO-labeled cells are detected with positive contrast by subtracting a susceptibility-weighted echo-time encoding technique (SWEET) image from a conventional spin-echo image [11]. Based on the subtraction from the spin-echo image, the SWEET technique can detect the location of SPIO-labeled cells under the influence of the susceptibility effect and to display them in positive contrast.

In order to separate the magnetic susceptibility effect from other off-resonance effects such as the main magnetic field inhomogeneity or chemical shift artifacts, SWEET utilizes the feature that the magnetic susceptibility effects arising from the SPIO-labeled cells are more profound and abrupt across the voxel, while the main magnetic field inhomogeneity varies slightly within an imaging voxel [11]. On the other hand, the chemical shift for water and fat is discrete and can be estimated for a given magnetic field strength (chemical shift difference between water and fat is $\delta_k=3.5$ ppm). Therefore, local field inhomogeneity caused by the presence of SPIO can be measured by shifting the 180° refocusing pulse (thus shifting the echo time) without adjusting the data acquisition window (the detailed theoretical framework of the SWEET method has been described elsewhere [11]).

The scope of this study was to implement a positive contrast technique using SWEET for cellular MRI and to verify its feasibility through *in vitro* phantom and *in vivo* mice imaging. A human epidermal carcinoma (KB) cell line was chosen for labeling due to its fast cell migration and proliferation in both *in vitro* and *in vivo* conditions. Gelatin phantoms containing various concentrations of the labeled cells were used to verify the method *in vitro*. The SPIO-labeled KB cells were also injected into the dorsal flanks (subcutaneously) as well as the hind limbs (intramuscularly) of nude mice to examine the efficacy of the proposed method in imaging the labeled cells *in vivo*. The tumor growth from the injected cancer cells was then imaged, and the presence of the SPIO-labeled cells was cross examined with histological sections.

2. Materials and methods

2.1. Cell labeling and phantom preparation

In order to verify the proposed method, human nasopharyngeal epidermal carcinoma (KB) cells (20,000 cells/cm²) were cultured in a 10% fetal bovine serum RPMI (Roswell Park Memorial Institute) medium (supplemented with 100 U/ml of penicillin and streptomycin) at 37°C. The cell labeling solution was prepared using 750 µg of SPIO (marketed under the name Feridex, Berlex, Inc., Wayne, NJ,

USA, or Endorem, Guerbet, Paris, France), 11.25 µg of poly-L-lysine (PLL, Sigma) and 15 ml of serum-free RPMI medium. The cells were incubated for 24 h at 37°C with the labeling solution to allow internalization [1] and were subsequently washed three times with fresh phosphate-buffered saline (PBS) to remove the residual extracellular SPIO or PLL. In order to visualize intracellular SPIO, cells were stained with Prussian blue solution (for iron staining) and propidium iodide solution (50 µg/ml in PBS; for cell nucleus staining). Optical images were then acquired using a confocal laser scanning microscope (LSM150, Carl Zeiss, Germany).

After magnetic labeling, the number of viable cells was determined via a cell counting kit [Cell counting kit-8 (CCK-8), Dojindo Laboratories, Kumamoto, Japan] for cell viability assay. SPIO-labeled KB cells were seeded in a six-well plate at a density of 3×10^4 cells/well and cultured at 37°C. The medium was exchanged daily, and the number of viable cells was counted after 1, 2, 3 and 4 days to examine the degree of proliferation. To ensure the reliability of the method, cell viability was also validated using a Trypan blue exclusion assay. Cell viability and proliferation were assessed in triplicate. The iron concentration within cells labeled with SPIO-PLL was quantified using inductively coupled plasma absorption emission spectroscopy (ICP-AES). For ICP-AES assay, the cell suspensions were diluted with a 22% HNO₃ solution, and then the obtained solution was nebulized into argon plasma.

Gelatin phantoms were constructed using 35-mm-diameter vials. Twelve milliliters of 10% (w/v) gelatin solution, pre-sterilized in an autoclave, was poured into each vial at 37°C. In order to place the group of cells in the middle of the well space, a tube-shaped gelatin groove was formed at the top-middle portion of the gelatin surface. SPIO-labeled KB cells were harvested and then resuspended in 10% (w/v) sterilized gelatin solutions with different concentrations. The cell–gelatin mixture (~10 µl in volume) was then poured in the groove using a micropipette. After fixation, an additional 3 ml of the sterilized gelatin solution was poured into the well to seal the labeled cell pellet. Phantoms containing cell pellets with seven different concentrations (5×10^3 , 1×10^4 , 5×10^4 , 1×10^5 , 2×10^5 , 5×10^5 and 1×10^6 cells/pellet) were prepared to examine the number of cells that could be detected by the proposed method and the relationship between cell concentration and the magnitude of the computed positive contrast. A control sample was prepared using 5×10^5 unlabeled KB cells.

2.2. Magnetic resonance imaging

MRI was performed on a 3.0-T MRI system (ISOL Tech., Korea) using a customized quadrature radiofrequency (RF) coil with a diameter of 9 cm for RF transmission and detection. Images of the *in vitro* phantom were obtained by a spin-echo pulse sequence using the following acquisition parameters: TR/TE=500/40 ms, FOV=80×80 mm², matrix=256×256, flip angle=90°, slice thickness=2 mm (no

gap), number of signal averages=2 and number of slices=5 (voxel size= $0.31 \times 0.31 \times 2$ mm³). First, a conventional spin-echo image was acquired as an anatomical reference with the above parameters. Subsequently, the SWEET sequence was implemented by a simple modification of the conventional spin-echo pulse sequence by changing the timing of the 180° refocusing pulse without adjustment of data acquisition window [11]. In order to extract the susceptibility effect of the SPIOs as a positive contrast signal, the susceptibility-weighted images with the echo-time shift were subtracted from the conventional spin-echo images (without echo-time shift). Moreover, in order to examine the effect of the echo-time shift, additional images with six different shifts (22.4, 17.92, 13.44, 8.96, 4.48 and 2.24 ms from the original TE) were acquired.

To examine the validity of the proposed method in monitoring the proliferation of SPIO-labeled cancer cells in an animal model, *in vivo* animal experiments were

conducted using mice (BALB/c nude mouse; $n=3$). All animal experiments were conducted in compliance with the guidelines set forth by the “Principles of Laboratory Animal Care” (by the National Institute of Health) [12]. Both SPIO-labeled and unlabeled KB cells were harvested and then resuspended in PBS with a concentration of 3×10^7 cells/ml. A 100- μ l aliquot of the cell suspension (therefore, 3×10^6 cells) was injected into two different locations: (1) subcutaneously to the left dorsal flank and (2) intramuscularly into the left hind leg. The corresponding right side was injected with unlabeled KB cells, which served as the control condition. MR images were acquired prior to injection of the cells as well as at eight postinjection time points [1 h after injection on Day 0, 1 day after injection (Day 1), Day 2, Day 4, Day 7, Day 9, Day 12 and Day 14] in order to monitor the proliferation of cancer cells and tumor growth. The imaging parameters for the reference anatomical image consisted of TR/TE=500/20 ms, 256×256

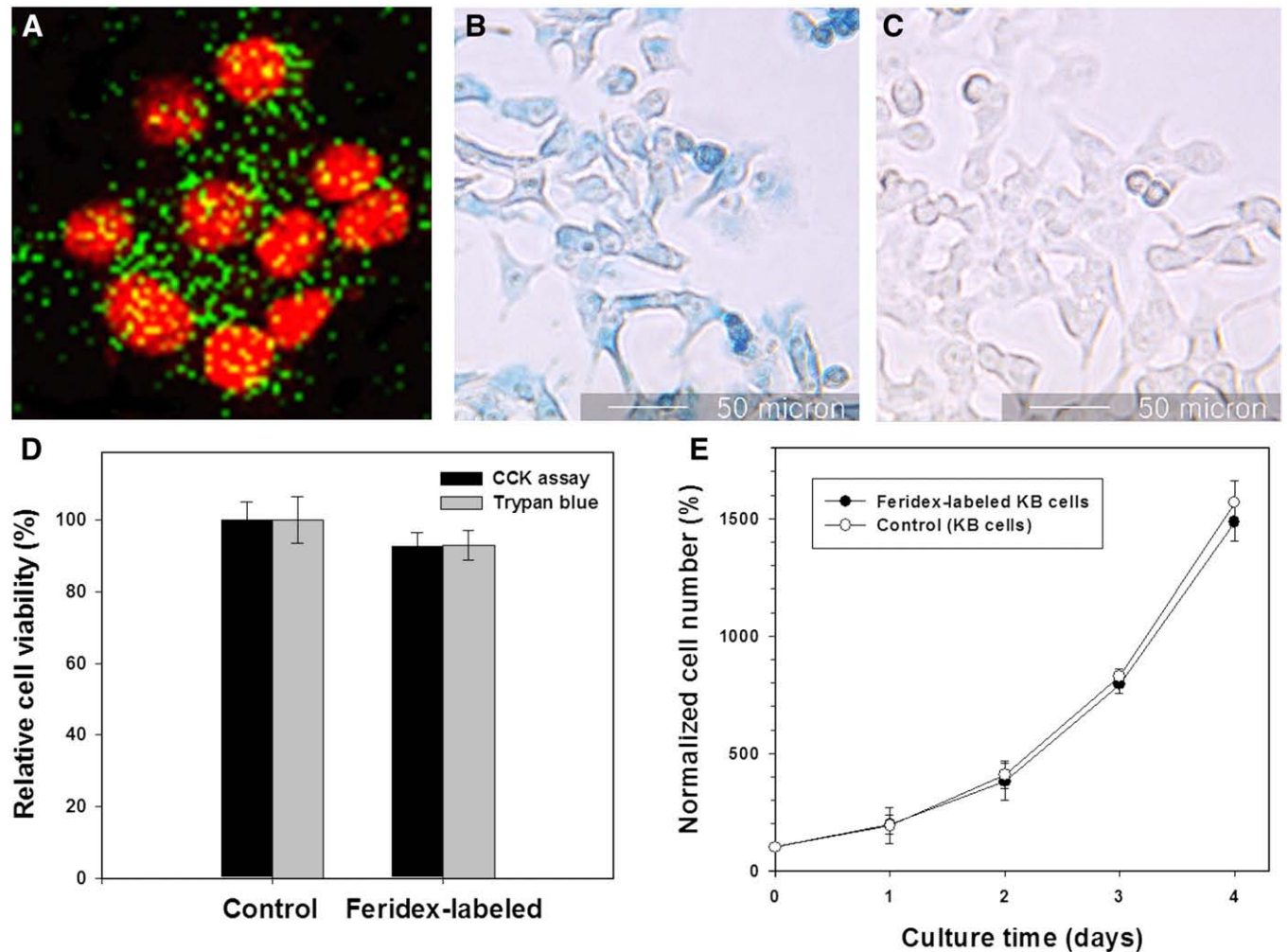


Fig. 1. (A) Confocal fluorescence microscopic image showing fluorescein-labeled SPIOs (in green) internalized into the KB cells. Nuclei were counterstained red. Prussian blue staining results of (B) SPIO-labeled KB cells and (C) unlabeled KB cells (control). (D) The results of two different methods of cell viability assays (CCK and Trypan blue dye) for both SPIO-labeled and control cells. (E) Cell proliferation in terms of the number of cells (normalized to the control at Day 0) as a function of the culture time (error bar shows the standard deviation of each case).

matrix, FOV of $100 \times 100 \text{ mm}^2$ and slice thickness of 3 mm (voxel size of $0.4 \times 0.4 \times 3 \text{ mm}^3$). An echo-time shift of 4.48 ms, which was the maximal value for TE=20 ms, was used for SWEET imaging. Different echo times were used for in vitro (TE=40 ms) and in vivo (TE=20 ms) imaging because T_2 of the in vitro sample is longer than that of the in vivo one. The amount of echo-time shift was adjusted accordingly to accommodate the position of 180° pulse before the acquisition window. Therefore, we used smaller echo-time shift (4.48 ms) for the in vivo than for the in vitro case (22.4 ms). The total acquisition time was 4 min for each set. In addition, the degree of difference between the reference and shifted-echo image was pseudo-colored and overlaid on the reference image after removal of image noise via thresholding with an adjustable cut-off value (1% of maximum intensity of the difference image).

After 2 weeks of MR imaging, a histological analysis was performed in order to validate the presence of MRI-detected SPIO-labeled cells. Mice were sacrificed and dissected to obtain tumor tissue for histological analysis. Tissue sections were stained with Prussian blue and neutral red counterstaining and observed/photographed using a Nikon TE300 inverted microscope equipped with a digital microscope camera (Polaroid DMC2, USA). An additional set of experiments were conducted to determine the sensitivity of the SWEET method for various cell concentrations. Different concentrations of SPIO-labeled KB cells (0.3×10^5 , 0.6×10^5 , 1.2×10^5 and 2.4×10^5) were placed in the hind legs of nude mice via muscular injection. One hour after injection, the three mice were imaged using the method and subsequent analysis techniques described above. This part of the experiment was conducted to

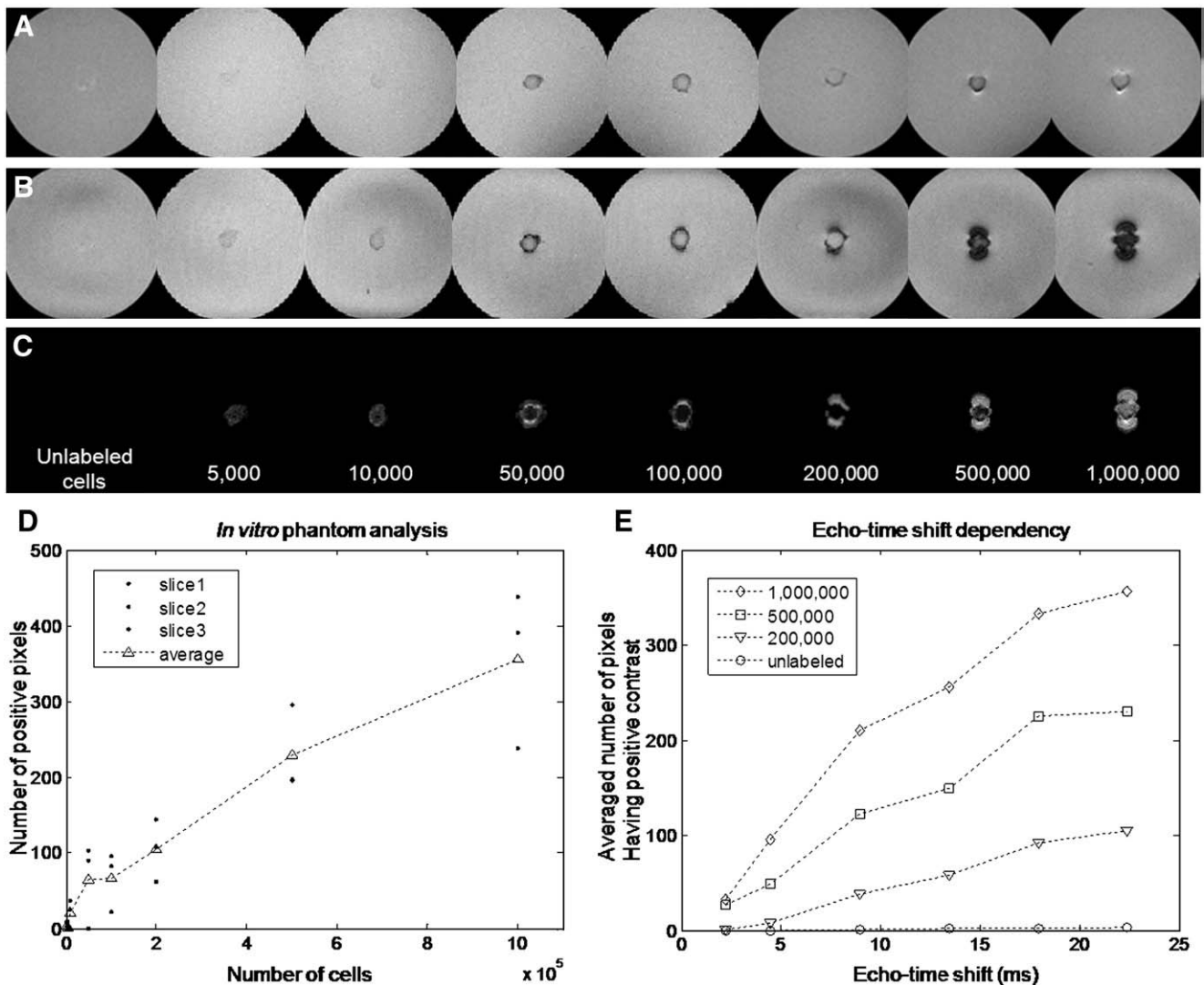


Fig. 2. In vitro gelatin phantom MR images and quantitative analysis for positive contrast imaging. (A) Spin-echo reference image, (B) susceptibility-weighted image using SWEET with an echo-time shift of 22.4 ms, (C) positive-contrast image in phantoms with varying numbers of cells [5×10^5 unlabeled cells (control) and 5×10^3 to 1×10^6 SPIO-labeled cells]. (D) The number of pixels showing positive contrast with respect to the number of labeled cells. (E) The average number of positive contrast pixels with respect to the echo-time shift for increasing cell concentration.

examine the sensitivity of the proposed method with respect to the number of SPIO-labeled cells for potential *in vivo* imaging applications.

3. Results

3.1. SPIO Uptake and cell viability assay

Confocal microscopic images of the Prussian blue stained cells (Fig. 1A) showed that SPIO particles, appearing as green fluorescent dots, were efficiently internalized into the cytoplasm. Strong red fluorescence was homogeneously distributed within the nucleus without any evidence of apoptosis (e.g., segregation and fragmentation of the cell

nucleus into dense and tiny granules [13]). SPIO-labeled KB cells were stained blue as a result of the uptake of iron oxide, while the unlabeled KB cells (control) were not stained (Fig. 1B and C). The viability of SPIO-labeled cells remained at 94% compared to that of the normal control (Fig. 1D), which is in close agreement with the results of previous investigations [14,15]. Importantly, SPIO labeling did not induce a significant decrease in the proliferation rate compared to the unlabeled cells (Fig. 1E).

3.2. *In vitro* phantom imaging

Fig. 2A shows the conventional spin-echo images of gelatin phantoms containing different cell concentrations of

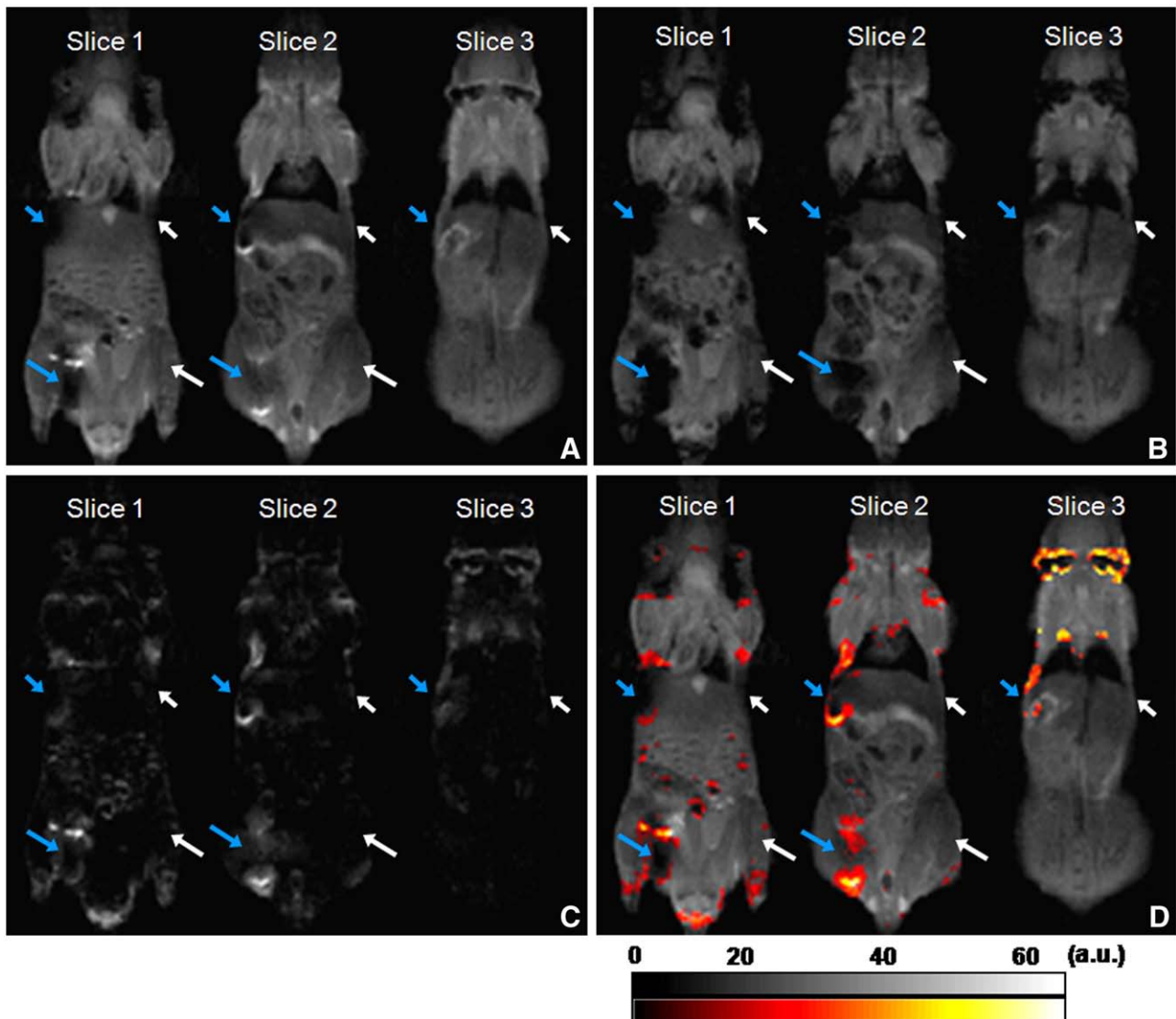


Fig. 3. *In vivo* MR images of a mouse at Day 1 upon cell injection (blue arrow indicates the injection site of SPIO-labeled cells, and the white arrow indicates the injection site of unlabeled cells). The cells were injected into dorsal flanks (short arrow) subcutaneously and the hind legs (longer arrow) intramuscularly. (A) Spin-echo reference images, (B) SWEET images, (C) positive-contrast images and (D) color-composite (scaled dark red to light yellow by normalizing the maximum value of each panel to 64) of positive contrast (as of Panel C) overlaid onto the spin-echo reference (as of Panel A) images. Injected sites on the left showed positive contrast due to the labeled SPIOs, while no apparent contrast was detected from the control sites (on the right). Note that the positive contrast detected from the ear and lung areas is due to the susceptibility effects from the air–tissue interface.

SPIO-labeled cell pellets and an unlabeled cell pellet. Fig. 2B shows corresponding susceptibility-weighted images obtained by SWEET with an echo-time shift of 22.4 ms. In each image, dark signal voids arising from SPIO-labeled cells are clearly apparent. Fig. 2C shows positive-contrast images generated from the difference between Fig. 2A and B (A minus B). As the number of labeled KB cells increased, the areas showing positive contrast also increased. As shown in Fig. 2D, the average number of pixels with positive contrast increased proportionally to the number of labeled cells. Fig. 2E illustrates that the number of positive-contrast pixels increased proportionally to the duration of the echo-time shift.

3.3. In vivo MR imaging

SPIO-Labeled KB cells implanted in nude mice (3 million cells per injection site) were clearly visualized using the proposed method. The conventional spin echo reference images (Fig. 3A) showed slight signal voids at the sites where SPIO-labeled KB cells were injected (left flank and hind leg, indicated by blue arrows). The echo-time shifted

images showed much larger signal voids near the SPIO-labeled cells, which were discriminated against the background tissue (in Fig. 3B). A positive-contrast image is shown in Fig. 3C, whose pseudo-color map is overlaid on its reference spin-echo image (in Fig. 3D). It is important to note that the strong susceptibility effect of the tissue–air interface around both ears is also visualized on the top of Slice 3. Fig. 4 shows spin-echo, echo-time shifted and positive contrast images of mice injected intramuscularly with 30,000 (A, left), 60,000 (A, right), 120,000 (B, left) and 240,000 (B, right) SPIO-labeled cells. It suggests that at least 30,000 SPIO cells can be successfully detected by the proposed method using clinically relevant imaging parameters.

Two weeks after injecting unlabeled and labeled KB cells, tumors of similar dimensions were found at all of the injected sites. Fig. 5A shows an example coronal spin-echo image of a mouse before injecting. Fig. 5B and C is the cropped images of the flank side and the hind leg, respectively. The positive-contrast area in the SPIO-labeled injection sites expanded to neighboring regions, indicating that the growth of labeled cells formed a tumor mass. Despite many cell divisions, daughter cells retained sufficient SPIO labeling to

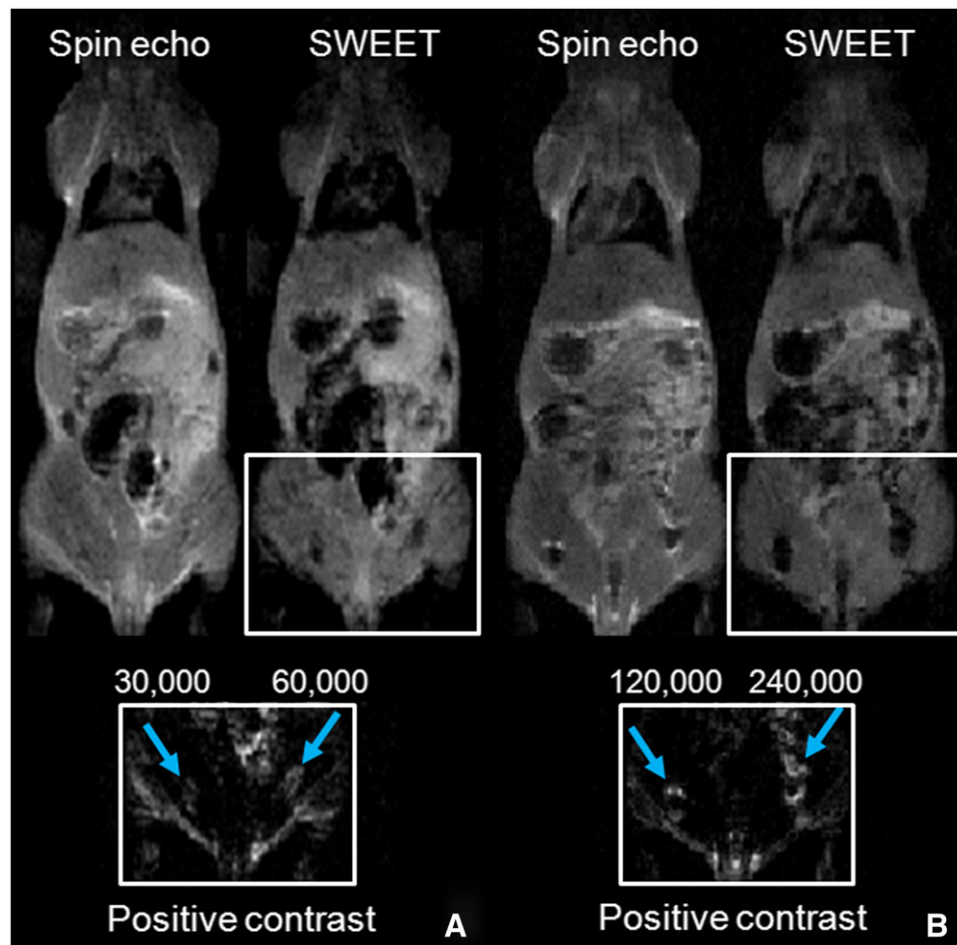


Fig. 4. Spin-echo, SWEET and positive contrast images show the minimum cell number detected by the proposed method. (A) and (B) show two mice which were intramuscularly injected with 30,000/60,000 and 120,000/240,000 SPIO-labeled cells, respectively.

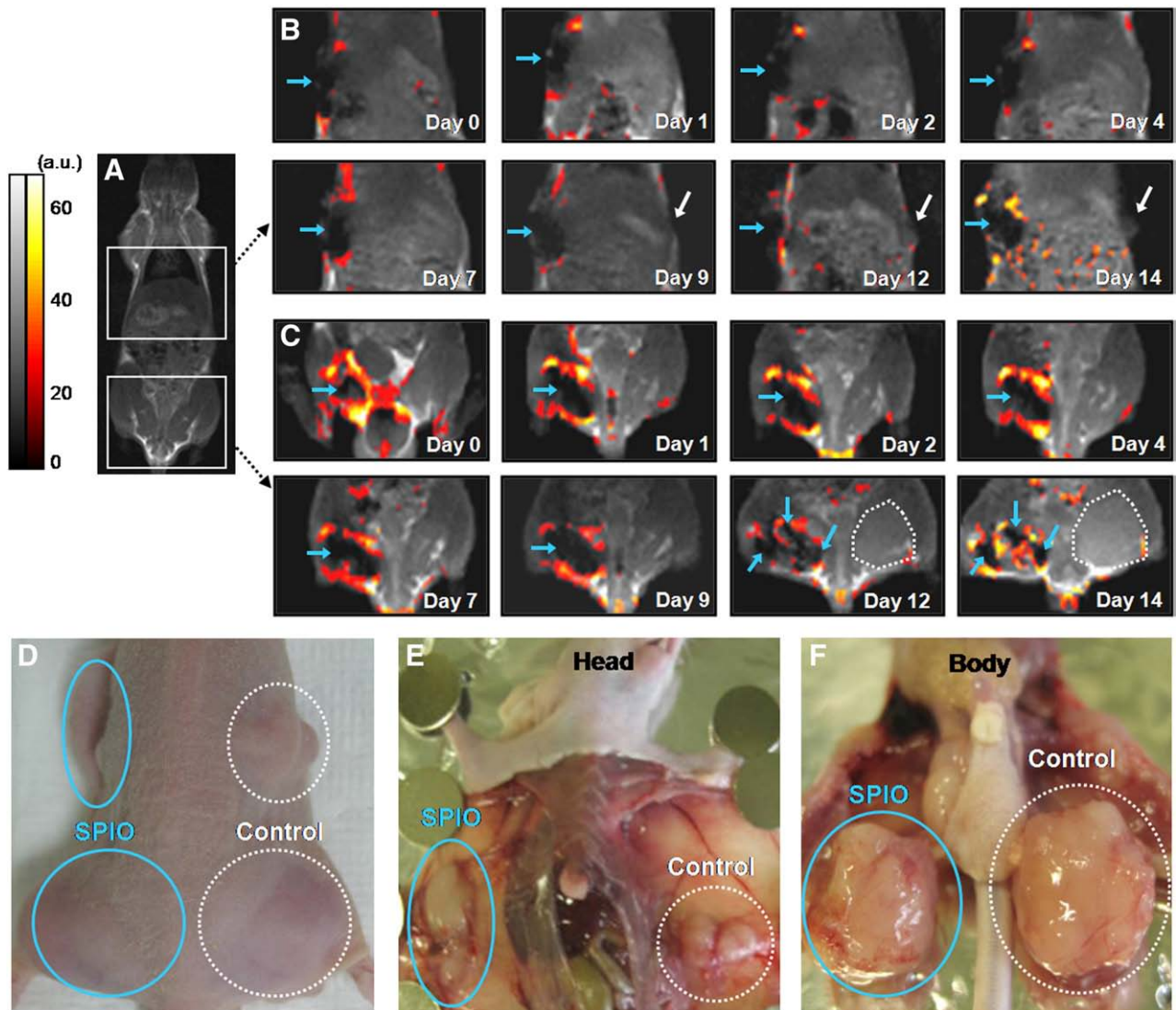


Fig. 5. Example spin-echo and SWEET images for a growing tumor over a 2-week period. Blue arrows and circles indicate the site of SPIO-labeled cells and white arrows and lines indicate the site of unlabeled cells as a control. (A) Selected anatomical slice scanned before cell injection. Panels indicate the magnified regions for the site of (B) subcutaneous injection and (C) intramuscular injection. After Day 9, the contrast between tumor tissue and normal tissue was shown at the control site (white dotted circles in right hind leg) with slight elevations in the signal. In addition, at Days 12 and 14, migration of SPIO-labeled cancer cells due to tumor growth was observed from the left leg (expanded dark region with blue arrows). (D) Outer appearance of tumor growth at Day 14 (before histological preparation). Dissection of the dorsal flanks (E) and hind legs (F) verifies tumor growth at the sites of cell injection.

generate positive contrast. After Day 9, positive contrast effect was reduced in Fig. 5C. This is likely due to the reduction of the number of proliferating labeled cells and the dumping of SPIOs occurring with cell necrosis. The tumor growth at the site of the injected SPIO-labeled and unlabeled (control) KB cells was evident (in Fig. 5D).

3.4. Histological analysis

After MR imaging for 2 weeks, the mice were sacrificed and dissected to collect tumor tissues at the site of the injection as shown in Fig. 5E and F. The reduction of the number of proliferating labeled cells at the site of the injected SPIO-labeled cells was evident (in Fig. 5F).

In close agreement with the above MR imaging results, the tumors originating from the SPIO-labeled cells in the subcutaneous layer (Fig. 6A) and the leg muscle (Fig. 6C) were selectively stained with Prussian blue, and the unlabeled tumor masses are shown in Fig. 6B and D.

4. Discussion

This study shows that the SWEET scheme can be exploited as a positive-contrast method for visualizing magnetically labeled tumor cells, whereby the positive contrast is manifested by the difference between the

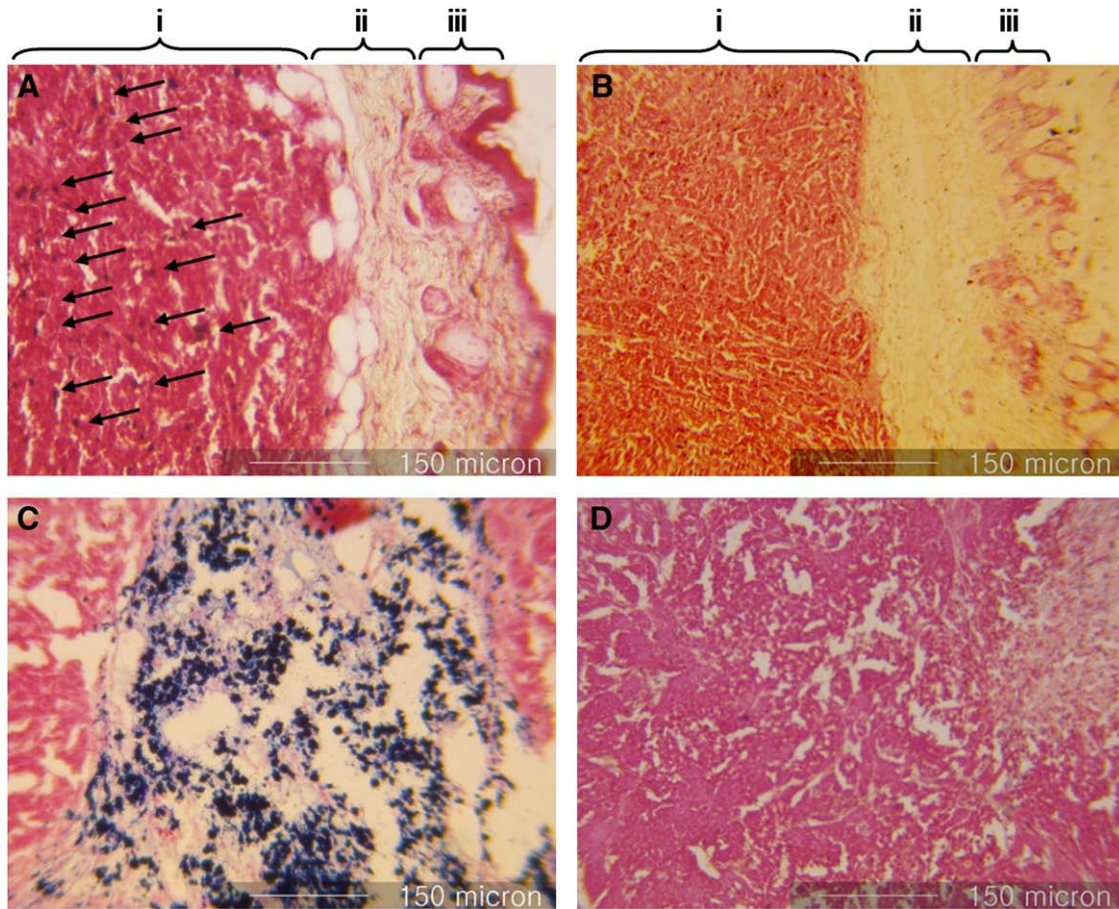


Fig. 6. Histological cross sections of tumor tissue stained with Prussian blue and neutral red counterstaining. Tumor sections from (A) the SPIO-labeled tissue (i: subcutaneous layer, ii: dermis, iii: epidermis) and (B) the control subcutaneous tissue. Sections of intramuscular tumor tissue from (C) a tumor originating from the SPIO-labeled cells and (D) the control site without labeling confirm the presence of SPIO particles within the tumor tissue (shown as blue dots).

conventional spin-echo images and the echo-time shifted images. The proposed method can be implemented with a simple modification of a conventional spin-echo sequence.

The experimental results have shown that the proposed method visualized a positive MR signal enhancement at the site injected with the labeled cells, as shown in Figs. 2 and 3. A crossed 'barbell'-like pattern could be observed in the region where the labeled cells were injected (in Slice 2 of Fig. 3C), reflecting the typical phase pattern formed around SPIO-labeled cells [16]. It was also found that the number of positive contrast pixels (above 10% of the maximum signal intensity of the subtracted image) increased proportionally with the number of labeled cells in each cell pellet (Fig. 2D). These results were also in good agreement with those of other studies, such as Cunningham et al. [6] and Stuber et al. [10], suggesting that the number of pixels detected by the susceptibility-weighted images can be used to indirectly estimate the number of labeled cells. Moreover, the number of pixels containing positive contrast is also proportional to the echo-time shift (from 2.24 to 22.4 ms as shown in Fig. 2E), which is in good agreement with the simulation results of Stables et al. [17] and is caused by the magnetic susceptibility effect around SPIO-labeled cells.

The shape and the spatial extent of the positive contrast tend to be greater than the region actually containing labeled cells. Unfortunately, this exaggeration is a limitation of positive contrast imaging methods. It would be difficult to model the exact extent of the positive contrast since the field inhomogeneity around the labeled cells was affected from the shape and the volume of injected space. However, the studies described herein investigated the relationship between the pixels with positive contrast and the number of injected cells for a given echo-time shift (22.4 ms) (see Fig. 2D), as well as its dependency on the echo-time shift (Fig. 2E). However, it is important to note that the extensive MR signature of the SPIO-labeled cells can be gainfully exploited to detect a single cell, and the detection of a single cell is warranted in cell-based therapies and cancer/stem cell monitoring [16].

The proposed method enabled the detection of SPIO-labeled cells in much lower numbers (in vitro for below 5000 up to 50,000 and in vivo for 30,000 cells as shown in Figs. 2 and 3) than in works reported by Cunningham et al. [6] (in vitro for 0.5 million and in vivo for 1 million cells) and Stuber et al. [10] (in vitro for 0.1 million and in vivo for 0.125 million cells). The proposed method, which does not require additional RF pulses for background suppression [10] or

frequency selection [6], is also advantageous in clinical settings with smaller RF power deposition. The method reported by Stuber et al. [10] can be adapted to spin-echo and gradient-echo sequences without heavy modification of the MR sequence; however, it would require additional adjustment of the bandwidth and angle of saturation pulse.

Since the proposed method is based on T_2^* weighting, gradient echo sequences could be alternatively used. However, the use of gradient-echo sequences, instead of the spin-echo sequences, would require separate imaging sessions for reference anatomical images using shorter TE compared to the ones for the cell detection, which results in different T_2 effect. Alternatively, a spin-echo sequence can be used to acquire anatomical information while the gradient-echo sequence is used to generate susceptibility-weighted images. In this case, the two sequences would have different slice profiles due to different RF pulse schemes. The use of spin-echo sequences in the SWEET technique can provide the same T_2 effect and the same slice profiles for both anatomical and T_2^* -weighted images for cell imaging. In addition, SWEET can be readily implemented with only minor sequence modifications of the timing of the 180° refocusing pulse.

The panels for Day 12 and Day 14 in Fig. 5C show that there are three distinct pools of SPIO particles, but the histology does not indicate that there are three pockets of proliferating viable tumor cells. The site of the unlabeled cells in the right flank and leg, however, showed a slightly elevated signal level rather than signal voids (shown as dotted circles). We postulate that this finding is due to the prolongation of T_2 relaxation time from edema around the tumor site [18]. It is also notable that the positive contrast was detected only at the rim of the tumor mass. This phenomenon may pose an intrinsic challenge in the use of SPIO-labeled cells for positive contrast imaging. This ‘blooming effect’ [19] with concomitant hypointensity at the actual position of the labeled cells is a common phenomenon for both positive and negative contrast imaging methods and was the case for the large number of iron-labeled cells observed in the work by Stuber et al. [10]. As evident from the imaging conducted on Day 12 and Day 14 (Fig. 5), the regions of positive contrast decreased over time in comparison to the initial cell injection. This decreased level of positive contrast can be attributed to the death (and concurrent release and absorption of SPIO particles to the body) or dilution of the intracellular SPIOs after cell proliferation and division [20,21] (see Fig. 6C). The MRI application of the method to track the SPIO-labeled cells, in terms of the duration of the traceability and the detection sensitivity, warrants further investigation and constitutes compelling subject for future studies.

Limitations of the current method include the restricted ranges for the amount of echo-time shift due to the position of the acquisition window for a given TE. Increasing echo-time shift would be accompanied by increased sensitivity toward magnetic susceptibility at the cost of signal loss and

an increased level of susceptibility artifacts. Another limitation of the proposed method is that it requires at least two data acquisitions to generate the desired positive contrast. However, the acquisition of conventional spin-echo images is routinely required in clinical practice for anatomical reference information.

In conclusion, this study showed that the SWEET method can be employed to selectively enhance the effect of the magnetic susceptibility caused by SPIO-labeled KB cells. It was also demonstrated that this method could be used to visualize SPIO-labeled KB cells and their tumor formation in mice for at least a 2-week period. Further study is needed to investigate the potential of this approach for application to in vivo monitoring of tumor metastasis and in the tracking of therapeutic cells (such as lymphocytes or stem cells) to tumor sites.

Acknowledgment

This work was partially supported by grants from the Korean Ministry of Commerce, Industry, and Energy (2004–02012), the Korean Ministry of Health and Welfare (02-PJ3-PG6-EV07-0002), and National Institutes of Health (NIH-RR019703).

References

- [1] Frank JA, Miller BR, Arbab AS, et al. Clinically applicable labeling of mammalian and stem cells by combining superparamagnetic iron oxides and transfection agents. *Radiology* 2003;228(2):480–7.
- [2] Walczak P, Kedziorek DA, Gilad AA, et al. Instant MR labeling of stem cells using magnetoelectroporation. *Magn Reson Med* 2005;54(4):769–74.
- [3] Zhu J, Wu X, Zhang HL. Adult neural stem cell therapy: expansion in vitro, tracking in vivo and clinical transplantation. *Curr Drug Targets* 2005;6(1):97–110.
- [4] Schultz JF, Kuhn JA, McCarty TM. Hepatic imaging with iron oxide magnetic resonance imaging. *Oncology* 2000;14:29–36.
- [5] Marzelli M, Fischer K, Kim YB, Mulkern R, Yoo S-S, et al. Composite MR contrast agents for conditioning cell-labeling. *Int J Imag Syst Tech* 2008;18(1):79–84.
- [6] Cunningham CH, Arai T, Yang PC, et al. Positive contrast magnetic resonance imaging of cells labeled with magnetic nanoparticles. *Magn Reson Med* 2005;53:999–1005.
- [7] Seppenwoolde JH, Viergever MA, Bakker CJ. Passive tracking exploiting local signal conservation: the white marker phenomenon. *Magn Reson Med* 2003;50:784–90.
- [8] Bakker CJ, Seppenwoolde JH, Vincken KL. Dephased MRI. *Magn Reson Med* 2006;55:92–7.
- [9] Mani V, Briley-Saebo KC, Itskovich VV, et al. Gradient echo acquisition for superparamagnetic particles with positive contrast (GRASP): sequence characterization in membrane and glass superparamagnetic iron oxide phantoms at 1.5 T and 3 T. *Magn Reson Med* 2006;55:126–35.
- [10] Stuber M, Gilson WD, Schar M, et al. Positive contrast visualization of iron oxide-labeled stem cells using inversion-recovery with on-resonant water suppression (IRON). *Magn Reson Med* 2007;58:1072–7.
- [11] Park HW, Ro YM, Cho ZH. Measurement of the magnetic susceptibility effect in high-field NMR imaging. *Phys Med Biol* 1988;33(3):339–49.
- [12] Principles of Laboratory Animal Care. NIH Publication 86-23. Bethesda, MD: National Institutes of Health; 1985.

- [13] Bacsó Z, Everson RB, Eliason JF. The DNA of Annexin V-binding apoptotic cells is highly fragmented. *Cancer Res* 2000;60:4623–8.
- [14] Kraitchman DL, Heldman AW, Atalar E. In vivo magnetic resonance imaging of mesenchymal stem cells in myocardial infarction. *Circulation* 2003;107:2290–3.
- [15] Kostura L, Mackay A, Pittenger MF, et al. Feridex labeling of human mesenchymal stem cells inhibits in vitro chondrogenesis. Proceedings of the 12th Annual Meeting of ISMRM, Kyoto; 2004 [abstract 167].
- [16] Heyn C, Bowen CV, Rutt BK. Detection threshold of single SPIO-labeled cells with FIESTA. *Magn Reson Med* 2005;53:312–20.
- [17] Stables LA, Kennan RP, Gore JC. Asymmetric spin-echo imaging of magnetically inhomogeneous systems: theory, experiment, and numerical studies. *Magn Reson Med* 1998;40:432–42.
- [18] Wessig C, Kenn W, Koltzenburg M, Bendszus M. Denervation hypertrophy may mimic local tumor spread on magnetic resonance imaging. *Muscle Nerve* 2006;34:108–10.
- [19] Kawashima A, Sandler CM, Ernst RD, et al. Imaging of non-traumatic hemorrhage of the adrenal gland. *Radiographics* 1999;19:949–63.
- [20] Wakczak P, Kedziorek DA, Gilad AA, Barnett BP, Bulte JWM. Application and limitations of MR tracking of neural stem cells with asymmetric cell division and rapid turnover: the case of the shiverer dysmyelinated mouse brain. *Magn Reson Med* 2007;58:261–9.
- [21] Lepore AC, Wakczak P, Rao MS, Fischer I, Bulte JWM. MR Imaging of lineage-restricted neural precursors following transplantation into the adult spinal cord. *Exp Neurol* 2006;201:49–59.